Alternating brittle and ductile response of coherent twin boundaries in nanotwinned metals

Tanushree Sinha and Yashashree Kulkarni[a)]
Department of Mechanical Engineering, University of Houston, Houston, Texas 77204, USA

Nanotwinned metals have opened exciting avenues for the design of high strength and high ductility materials. In this work, we investigate crack propagation along coherent twin boundaries in nanotwinned metals using molecular dynamics. Our simulations reveal that alternating twin boundaries exhibit intrinsic brittleness and ductility owing to the opposite crystallographic orientations of the adjoining twins. This is a startling consequence of the directional anisotropy of an atomically sharp crack along a twin boundary that favors cleavage in one direction and dislocation emission from the crack tip in the opposite direction. We further find that a blunt crack exhibits ductility in all cases albeit with very distinct deformation mechanisms and yield strength associated with intrinsically brittle and ductile coherent twin boundaries. © *2014 AIP Publishing LLC*. [http://dx.doi.org/10.1063/1.4901472]

I. INTRODUCTION

Twin boundaries (TBs) have sparked renewed interest in recent years owing to their role in governing the remarkable properties of nanotwinned structures.[1–12] Some of these properties revealed through extensive experimental studies and mechanistic modeling include ultra-high yield strength, enhanced ductility, strain rate sensitivity, and grain stability. It is well established that TBs in nanotwinned metals serve as effective barriers for dislocation motion, thus constituting a strengthening motif, and also serve to accommodate large plastic strains by absorbing dislocations leading to enhanced ductility.[13–16] Recent experimental and computational studies have also investigated the fracture and failure mechanisms in these materials.[17–24] Several studies have revealed an improved fracture resistance of nanotwinned structures due primarily to the interaction of coherent twin boundaries (CTBs) with cracks and dislocations nucleating from crack tips.[17–20] A recent experimental study has shown an interesting ductile-to-brittle transition in Au nanowires with decreasing twin spacing on the order of a few angstroms.[21] They attribute it to the transition from heterogeneous dislocation nucleation from free surfaces at large TB spacing to homogeneous nucleation along CTBs at small TB spacing which leads to a brittle-like behavior. In contrast, another experimental study has reported a brittle-to-ductile transition with decreasing twin spacing in twinned Cu nanowires with angstrom-scale twins.[22] According to this work, the CTBs are found to have an intrinsic tendency for cleavage in the CTB plane which, for very small twin lamella, is dominated by dislocation nucleation at nearby CTBs leading to plastic behavior. The distance of the crack tip from a CTB has also been shown to cause an interesting alternating brittle and ductile behavior of nanotwinned metals.[23] These studies taken together suggest that various competing mechanisms, size effects, and material properties govern the overall fracture response of nanotwinned structures. In this work, we investigate the propagation of pre-existing cracks along CTBs to elucidate their fracture response owing to the effect of the crystallographic orientations in the adjoining twins. We note that although some recent works suggest that CTBs are intrinsically brittle,[22] a systematic study of the geometric constraints that lead to the intrinsic fracture response of CTBs has not been reported. Interestingly enough, our simulations reveal that CTBs exhibit alternating brittle and ductile behavior. These findings can provide insight into the intriguing twin-spacing dependent transition between brittle and ductile behavior of nanotwinned metals and the brittleness of CTBs observed in recent works.

II. SIMULATION METHOD

Simulations were performed on bicrystals and nanotwinned specimens using the embedded-atom-method (EAM) potential for copper developed by Mishin *et al.*[25] The specimens were aligned along the $[1\bar{1}0]$, $[11\bar{2}]$, and $[111]$ crystallographic directions with periodic boundary conditions applied only in the $[1\bar{1}0]$ direction (Figure 1). Each specimen consisted of about 161,000 atoms with dimensions of $4\,nm \times 10\,nm \times 40\,nm$ and contained a pre-existing edge crack which was atomically sharp. The crack was located on a CTB plane with the crack front along the $[1\bar{1}0]$ direction and its length was half the width of the specimen. As shown in Figure 1(a), the grain above the CTB in the bicrystal has the original orientation and is denoted by "M" as the matrix, while the grain below the CTB is denoted by "T" as the twin or the mirror image. For the sake of convenience, we refer to such a CTB as positive (+). In nanotwinned specimen, a CTB with twin orientation above and matrix orientation below is referred to as negative (−). The nanotwinned specimen shown in Figure 1(b) has a twin boundary spacing of 1.25 nm. The specimens were generated by incorporating the thermal expansion in the lattice spacing at 300 K and then equilibrating for 50 ps under the NPT

a)Electronic mail: ykulkarni@uh.edu
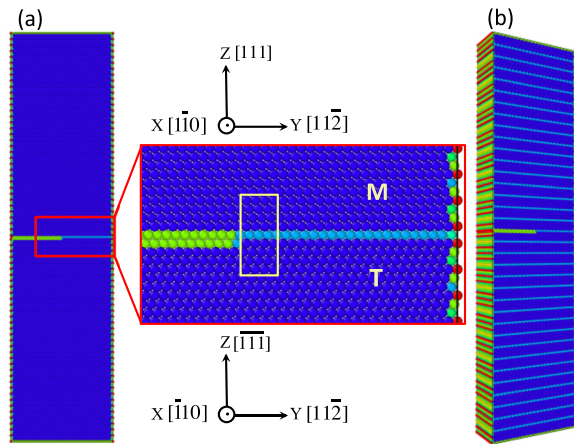
FIG. 1. Crystallographic orientation of the specimen used in the simulations. (a) Bicrystalline specimen with a pre-existing crack along the CTB (also shown in the zoomed in view). The yellow box at the crack-tip shown in the close-up view defines the region used in the local virial stress calculations. (b) Nanotwinned specimen with twin spacing of 1.25 nm and a pre-existing crack along a CTB.

ensemble using the Nosé-Hoover thermostat. Tensile loading was applied under the NVT ensemble by moving the top few layers of atoms at a constant velocity of 0.02 Å/ps while keeping the bottom few layers of atoms fixed (see Ref. 26 for details). The applied strain rate was $4.75 \times 10^7 \, \text{s}^{-1}$. All simulations were performed using LAMMPS,[27] and the atomistic structures were visualized based on the centro-symmetry parameter using OVITO.[28]

III. RESULTS AND DISCUSSION

Figures 2(a) and 2(b) show the evolution of the atomically sharp crack on positive and negative CTBs, respectively, in a nanotwinned specimen under mode I loading. When the crack is on a positive CTB, it propagates via cleavage along the CTB. However, when the crack is located on an adjacent (negative) CTB, it favors dislocation emission from the crack tip. To understand this contrasting behavior of different CTBs, we examine the crystal structure at crack tips on positive and negative CTBs as illustrated in Figure 3 and compare the energetic costs for different mechanisms. The red lines mark the projections of the {111} slip planes emanating from the crack tip into the matrix and the twin. We note that the actual slip systems available on a CTB can be represented as an octahedron with the CTB forming the common face of the two Thompson tetrahedra above and below the twin plane (see Figure 2 in Ref. 29). However, due to periodic boundary conditions, only the slip planes parallel to the [110] direction which is the direction of the crack tip (and periodicity) can be activated.[31–34]

According to Griffith's theory of fracture,[30] the energy release rate for brittle crack propagation along the CTB is given by

$$G_{cleav} = 2\gamma_s - \gamma_{CTB}, \tag{1}$$

where γ_s is the energy required to create a free surface and γ_{CTB} is the energy of the CTB. Based on the classical model by Rice for dislocation nucleation at an atomically sharp
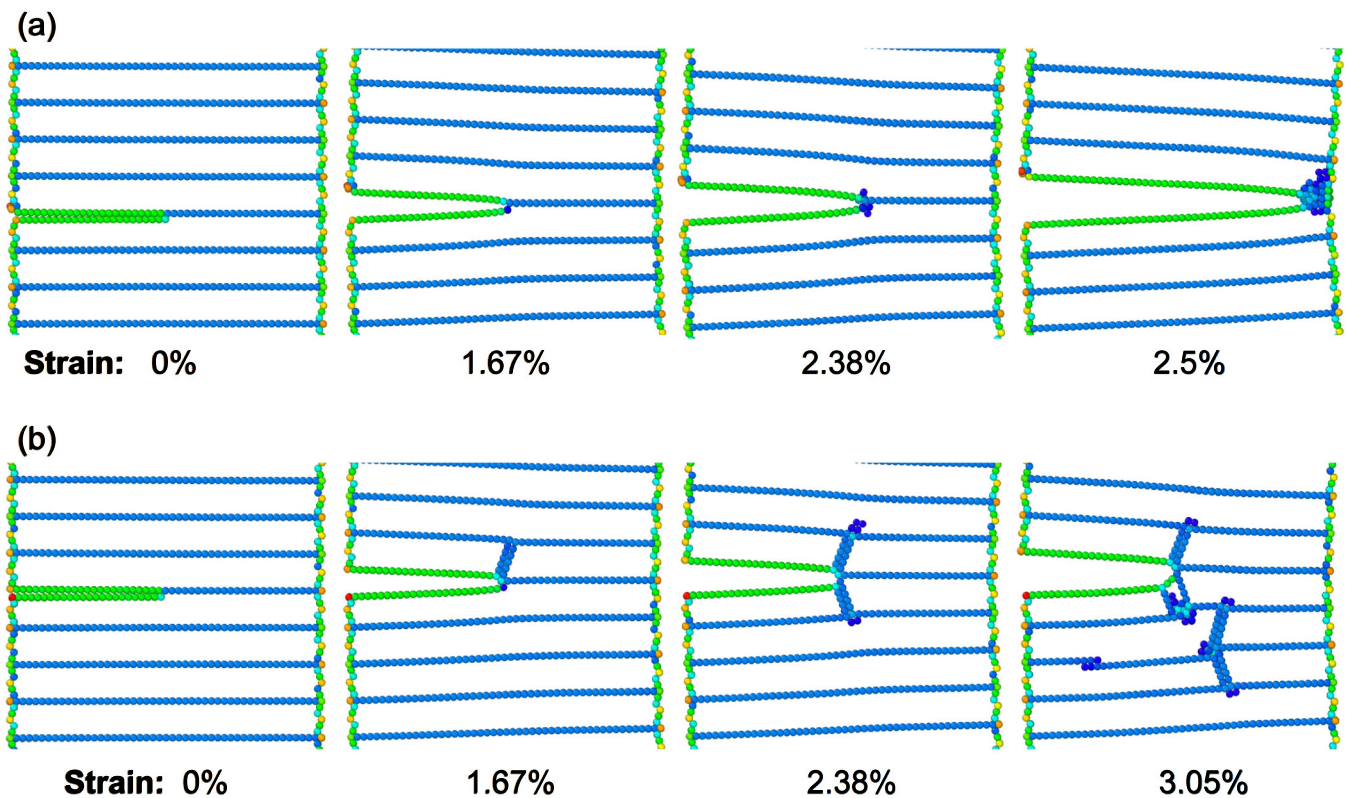
FIG. 2. Evolution of a crack along (a) positive CTB and (b) negative CTB in a nanotwinned specimen under mode I loading. Atoms are displayed according to the centrosymmetry parameter. Atoms in perfect fcc structure are not shown. The crack along the positive CTB shows brittle behavior, while the crack along the negative CTB shows ductile behavior.
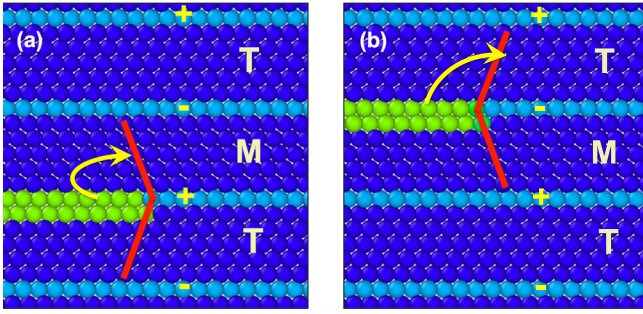
FIG. 3. (a) Crack located on a + CTB with matrix "M" orientation above and twin "T" orientation below. (b) Crack located on a − CTB with "T" orientation above and "M" orientation below. The red lines mark the projections of the {111} planes in the matrix and the twin. The atoms on the crack are shown in green, the hcp (CTB) atoms are shown in light blue, and the fcc atoms are shown in dark blue color.

crack tip,[31] the energy release rate for dislocation nucleation under mode I loading is given by

$$G_{disl} = 8\gamma_{usf}[1 + (1-\nu)\tan^2\phi]/[(1+\cos\theta)\sin^2\theta], \quad (2)$$

where γ_{usf} is the unstable stacking fault energy, ν is the Poisson's ratio, θ is the inclination angle of the slip plane with respect to the crack, ϕ is the angle of the Burgers vector with respect to a line in the slip plane normal to the crack front (see Figure 7 in Ref. 31). Table I compares the energetic costs for brittle cleavage and dislocation nucleation along the different possible slip planes marked by red lines in Figure 3. Thus, it is much more energetically favorable to emit partial dislocations in the "forward" direction shown in Figure 3(b) than the "backward" direction shown in Figure 3(a). This is because the leading partial in the forward direction has a pure edge character, whereas a leading partial in the backward direction would have a large screw component which is energetically less viable under mode I loading.[33,34] The table also shows that the energy release rate for brittle cleavage along a CTB in Cu lies between the energetic costs for dislocation nucleation in the backward and forward directions. As a consequence, the crack on a positive CTB shows the formation of an embryonic dislocation at the crack tip that becomes energetically too expensive and the crack ultimately propagates by decohesion. The crack on a negative CTB evolves by emitting {111}⟨112⟩ Shockley partials in the adjacent twins leaving behind stacking fault ribbons, which is the signature of incipient plasticity in ductile fcc metals.[8,17,24] This opposite response of cracks along positive and negative CTBs was observed in a series of simulations

TABLE I. Comparison of energy release rate for brittle cleavage and dislocation nucleation along the slip planes indicated by red lines in Figure 3. The values of the parameters ν, γ_{usf}, γ_s, and γ_{CTB} are taken from the work of Cheng et al.[33] The Poisson's ratio is obtained from typical experimental values, and the rest of the parameters are calculated based on the same interatomic potential used in our study.

CTB	θ	ϕ	ν	γ_{usf} (J/m²)	γ_s (J/m²)	γ_{CTB} (J/m²)	G_{disl} (J/m²)	G_{cleav} (J/m²)
+	109.47	60	0.324	0.158	1.239	0.022	6.458	2.457
−	70.53	0	0.324	0.158	1.239	0.022	1.067	2.457

on nanotwinned specimen with same sample dimensions described above and twin lamella thickness ranging from 0.6 nm to 15 nm.

We note that Cheng et al.[33] have observed a similar contrasting response of a crack along a CTB on reversing its direction. For the specimen and crack orientations shown in Figure 1, when the crack is directed along the positive Y-direction (the crack is on the left), it propagates via cleavage along the CTB, whereas when the direction of the crack is reversed (the crack is on the right), it favors dislocation emission from the crack tip (see Figure S1 in Supplemental Material[38]). Based on the reasons discussed above and illustrated in Figure S2 in Supplemental Material,[38] Cheng et al. attribute this behavior to the directional anisotropy resulting from the different crystallographic orientations of the matrix and the twin. Thus, as a rather intriguing consequence of this directional anisotropy of fracture along CTBs, our study demonstrates that alternating CTBs exhibit intrinsic brittleness and ductility.

In order to examine the effect of the atomically sharp crack tip on the brittle-ductile response of alternate CTBs, we also repeated these simulations for a slightly blunt crack that was created by removing a half-layer of atoms. As shown in Figure 4(b), the crack on a negative CTB continues to deform via emission of partial dislocations in the upper and lower grains due to activation of the two favorable slip systems. However, the crack on a positive CTB is no longer perfectly brittle but exhibits dislocation emission, unlike the atomically sharp crack discussed above. This is consistent with the observation of Schiøtz, et al.[36] that blunting a crack tip even by an atomic layer can cause a brittle-to-ductile transition by making it easier to emit a dislocation. Nonetheless, it is evident from the defect structures (Figures 4(a) and 4(b)) and the distinct stress-strain curves (Figure 6(a)) that although both specimen with blunt cracks exhibit plasticity, the deformation mechanisms are drastically different.

Figure 4(a) shows that due to the suppression of the favorable {111} slip planes at the intrinsically brittle crack tip, the crack propagates slightly and then nucleates a perfect $\frac{1}{2}(001)\langle\bar{1}\bar{1}0\rangle$ dislocation. After impinging on the adjacent CTB, it is subsequently transmitted into the adjacent twin as a Shockley partial, leaving a Frank partial at the twin-slip intersection. The dissociation is shown by the following reaction also discussed in Refs. 8 and 24, and illustrated in Figures 5(a) and 5(b):

$$\underbrace{\frac{1}{2}(001)\langle\bar{1}\bar{1}0\rangle}_{\text{Unit dislocation}} = \underbrace{\frac{1}{6}(\bar{1}1\bar{1})\langle1\bar{2}\bar{1}\rangle}_{\text{Shockley partial}} + \underbrace{\frac{1}{3}(112)\langle11\bar{1}\rangle}_{\text{Frank partial}}. \quad (3)$$
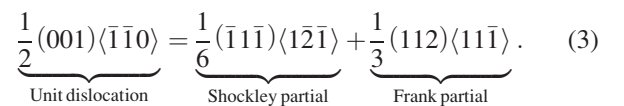
On the other hand, Figure 4(b) shows that plasticity initiates with the nucleation of the leading Shockley partial from the intrinsically ductile crack tip leaving behind a stacking fault ribbon. The leading partial impinges upon the adjacent CTB and undergoes the following dislocation reaction which is illustrated in Figures 5(c) and 5(d):

$$\underbrace{\frac{1}{6}(11\bar{1})[1\bar{2}\bar{1}]}_{\text{leading partial}} = \underbrace{\frac{1}{6}(111)[2\bar{1}\bar{1}]}_{\text{DSC partial}} + \underbrace{\frac{1}{6}(001)[\bar{1}\bar{1}0]}_{\text{stair-rod dislocation}}. \quad (4)$$
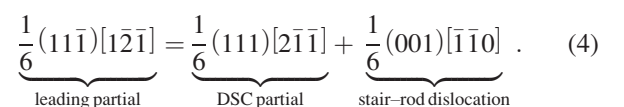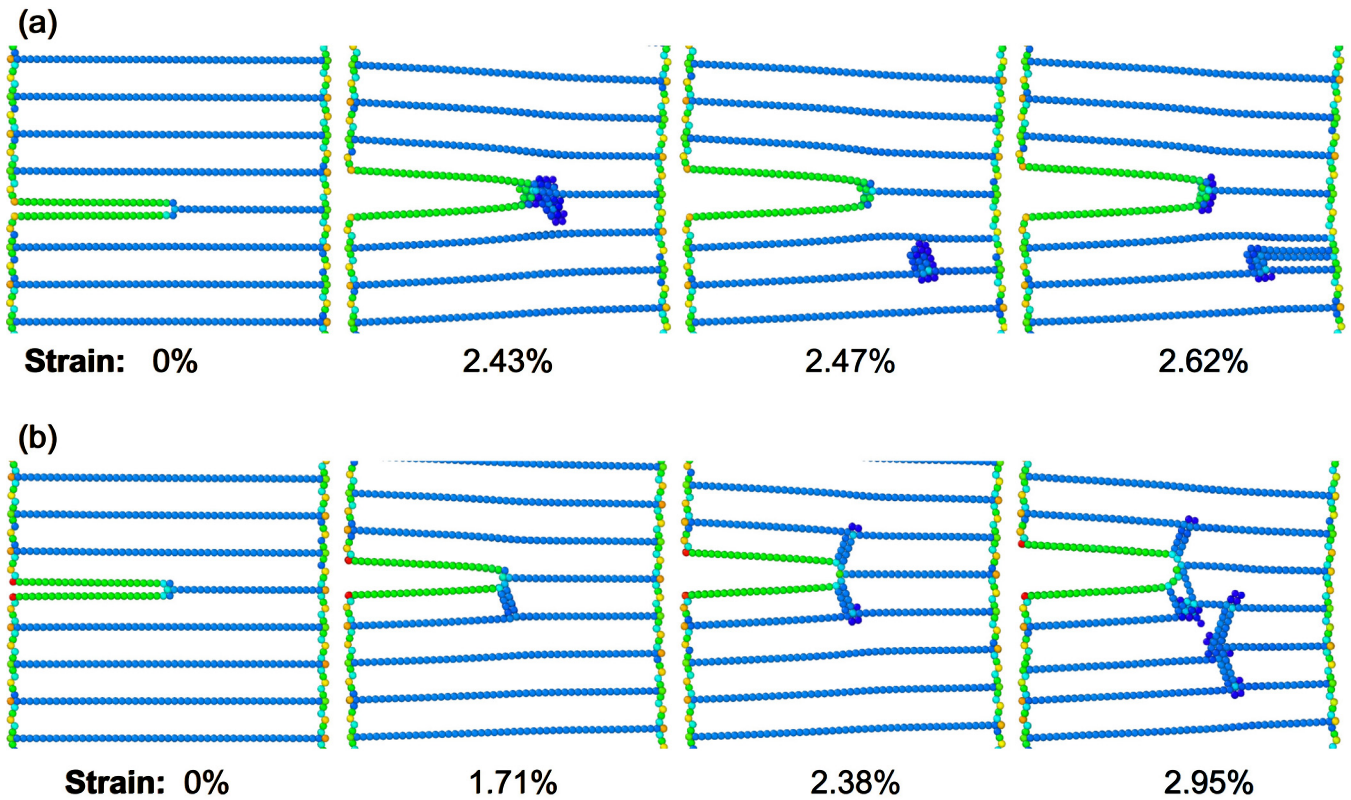
FIG. 4. Evolution of a blunt crack along (a) positive CTB and (b) negative CTB in a nanotwinned specimen under mode I loading. The two cases, although ductile, show very different deformation mechanisms.

The dissociation leaves a glissile displacement shift complete (DSC) partial dislocation on the twin plane and a stair-rod dislocation pinned at the twin-slip intersection. This

FIG. 5. (a) and (b) show a perfect dislocation emitted from the intrinsically brittle crack tip which is transmitted into the adjacent twin as a Shockley partial, leaving a Frank partial at the twin-slip intersection. (c) and (d) show a Shockley partial emitted from the intrinsically ductile crack tip which forms a twin partial (or DSC partial) and a stair-rod dislocation at the twin-slip intersection. Red indicates hcp atoms, blue indicates bcc atoms.

results in the formation of a Lomer-Cottrell lock, which is an important strain hardening mechanism,[35] and has been observed in several prior atomistic simulations on nano-twinned metals (see, for example, Ref. 8).

Figure 6(a) reveals that the stress-strain curve for the intrinsically ductile (−) CTB shows significant strain hardening for both sharp as well as blunt cracks with the ultimate strength being about 3.5 GPa. This is almost 1.5 GPa higher than the yield strength for these specimen and is attributed to the formation of Lomer-Cottrell locks. It is also interesting to note that although the blunting changes the response of the intrinsically brittle (+) CTB from cleavage to dislocation emission, there is hardly any change in the yield strength (about 2.6 GPa) and no strain hardening is observed. Thus, compared to the emission of Shockley partials observed at a typical ductile crack tip, this dislocation nucleation process is still energetically prohibitive and occurs only due to the suppression of the favored slip systems. Comparing the evolution of the local stresses for the different cases in Figure 6(b), we find that the stress concentration at the crack tip on the intrinsically ductile CTB is quite lower than the intrinsically brittle CTB. Moreover, comparing the local stress at the sharp and blunt crack tip on the intrinsically brittle CTB shows indiscernible difference in stress concentration. Taken together, we conclude that the blunting process leads to a surprisingly modest change in the stress concentration albeit sufficient to drive the brittle-to-ductile transition. This is consistent with the observation made by Schiøtz and coworkers[34,36] on comparing sharp and blunter (wedge-shaped) cracks.
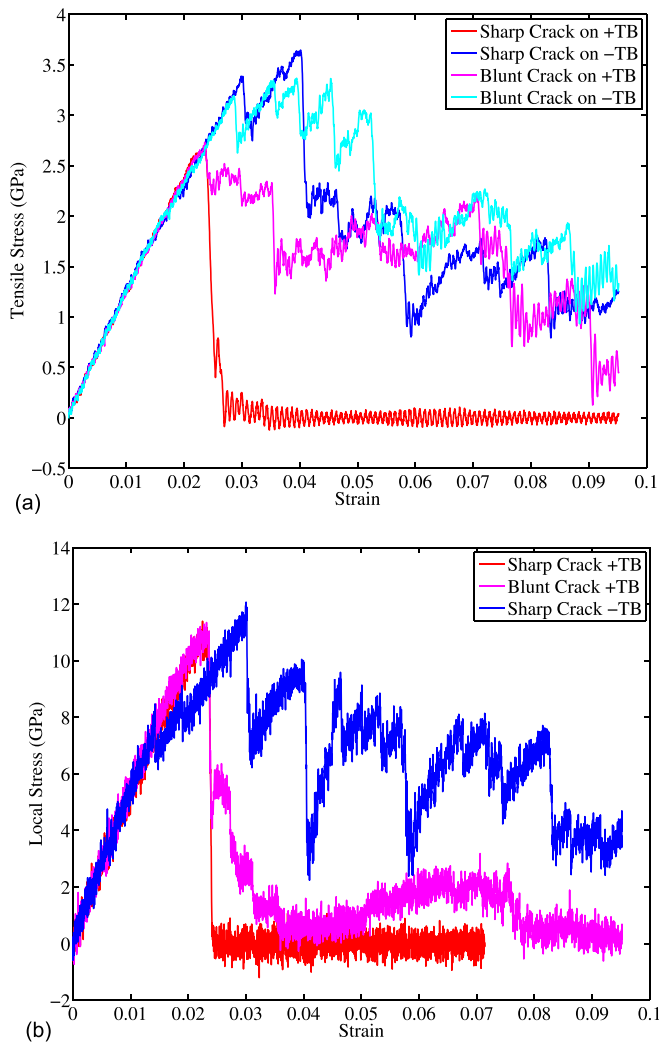
FIG. 6. (a) Tensile stress versus strain curves for nanotwinned specimen comparing the response of sharp and blunt cracks on positive and negative CTBs. (b) Local virial stress at the crack tip versus strain for the sharp and blunt cracks.

IV. CONCLUSION

In conclusion, our atomistic simulations reveal that CTBs in nanotwinned structures exhibit alternating intrinsic brittleness and intrinsic ductility. Since most of the research till date has focused on the overall response of nanotwinned specimen, this intriguing characteristic of alternating CTBs has not been reported before. Despite Cu being a ductile material, the brittle response stems from the suppression of energetically favored slip planes for dislocation emission. This is consistent with earlier predictions that cleavage could be made to occur at interfaces in layered ductile materials via dislocation confinement.[37] Our findings can throw light on some of the studies of the brittle versus ductile response of nanotwinned metals reported in recent literature. For instance, the brittle fracture observed in the simulations by Jang *et al.* (Figure S13 in Ref. 22) for nanotwinned specimen with 4.3 nm TB spacing, is found to occur on a positive CTB which is indeed intrinsically brittle according to our study. Similarly, the intragranular brittle cleavage along a CTB observed by Zhou and Qu (Figure 3 in Ref. 18) and Sun

et al. (Figure 2 in Ref. 24) seems to occur along a positive CTB. In fact, as a manifestation of the directional anisotropy, our simulations of a pre-existing blunt elliptical crack in polycrystalline nanotwinned Cu with columnar grains show the crack propagating via cleavage at the intrinsically brittle crack tip on one end and emitting dislocations from the intrinsically ductile crack tip on the other end.[38] Our results could also explain the surprising brittle-like deformation of the crack-tip near alternating CTBs observed by Liu *et al.*[23] It bears emphasis that the contrasting behavior of alternating CTBs is an intrinsic characteristic of the CTBs owing to the different crystallographic orientations of the adjoining twins and may often be dominated by other competing mechanisms. We have already discussed the transition from brittle cleavage to a more ductile response by blunting a sharp crack on an intrinsically brittle CTB. It was also observed in some of our simulations (not discussed here) that removing the periodic boundary conditions in the $[1\bar{1}0]$ direction allows the activation of other $\{111\}$ slip systems (Figure 2 in Ref. 29), leading to a ductile response of a crack on any CTB albeit by partial nucleation on different slip planes. The effects of the crack-length, material properties, and strain rate are some other important avenues that warrant further experimental and computational investigations.

[1]K. Lu, L. Lu, and S. Suresh, Science **324**, 349 (2009).
[2]L. Lu, Y. Shen, X. Chen, L. Qian, and K. Lu, Science **304**, 422 (2004).
[3]A. G. Frøseth, P. M. Derlet, and H. Van Swygenhoven, Adv. Eng. Mater. **7**, 16 (2005).
[4]X. Zhang, H. Wang, X. H. Chen, L. Lu, K. Lu, R. G. Hoagland, and A. Misra, Appl. Phys. Lett. **88**, 173116 (2006).
[5]T. Zhu, J. Li, A. Samanta, H. G. Kim, and S. Suresh, Proc. Natl. Acad. Sci. U.S.A. **104**, 3031 (2007).
[6]A. M. Hodge, Y. M. Wang, and T. W. Barbee, Jr., Scr. Mater. **59**, 163 (2008).
[7]R. J. Asaro and Y. Kulkarni, Scr. Mater. **58**, 389 (2008).
[8]F. Sansoz, H. Huang, and D. H. Warner, JOM **60**, 79 (2008).
[9]C.-T. Lu and K. Dayal, Philos. Mag. Lett. **91**, 264 (2011).
[10]M. Demkowicz, O. Anderoglu, X. Zhang, and A. Misra, J. Mater. Res. **26**, 1666 (2011).
[11]D. Chen and Y. Kulkarni, MRS Commun. **3**, 241 (2013).
[12]H. Mirkhani and S. P. Joshi, J. Mech. Phys. Solids **68**, 107 (2014).
[13]M. Dao, L. Lu, Y. F. Shen, and S. Suresh, Acta Mater. **54**, 5421 (2006).
[14]A. J. Cao and Y. G. Wei, J. Appl. Phys. **102**, 083511 (2007).
[15]K. A. Afanasyev and F. Sansoz, Nano Lett. **7**, 2056 (2007).
[16]Y. Kulkarni, R. J. Asaro, and D. Farkas, Scr. Mater. **60**, 532 (2009).
[17]H. Zhou and S. Qu, J. Comput. Theor. Nanosci. **7**, 1931 (2010).
[18]H. Zhou and S. Qu, Nanotechnology **21**, 035706 (2010).
[19]S.-W. Kim, X. Li, H. Gao, and S. Kumar, Acta Mater. **60**, 2959 (2012).
[20]H. Zhang, Y. Fu, Y. Zheng, and H. Ye, Phys. Lett. A **378**, 736 (2014).
[21]J. Wang, F. Sansoz, J. Huang, Y. Liu, S. Sun, Z. Zhang, and S. X. Mao, Nat. Commun. **4**, 2768 (2013).
[22]D. Jang, X. Li, H. Gao, and J. R. Greer, Nat. Nanotechnol. **7**, 594 (2012).
[23]L. Liu, J. Wang, S. K. Gang, and S. X. Mao, Sci. Rep. **4**, 4397 (2014).
[24]L. G. Sun, X. Q. He, J. B. Wang, and J. Lu, Mater. Sci. Eng. A **606**, 334 (2014).
[25]Y. Mishin, M. J. Mehl, D. A. Papaconstantopoulos, A. F. Voter, and J. D. Kress, Phys. Rev. B **63**, 224106 (2001).

[26]T. Sinha and Y. Kulkarni, J. Appl. Phys. **109**, 114315 (2011).
[27]S. J. Plimpton, J. Comput. Phys. **117**, 1 (1995).
[28]A. Stukowski, Model. Simul. Mater. Sci. Eng. **18**, 015012 (2010).
[29]Z. X. Wu, Y. W. Zhang, and D. J. Srolovitz, Acta Mater. **57**, 4508 (2009).
[30]A. A. Griffith, Philos. Trans. R. Soc. London, Ser. A **221**, 163 (1921).
[31]J. R. Rice, J. Mech. Phys. Solids **40**, 239 (1992).
[32]T. Zhu, J. Li, and S. Yip, Phys. Rev. Lett. **93**, 025503 (2004).
[33]Y. Cheng, Z.-H. Jin, Y. W. Zhang, and H. Gao, Acta Mater. **58**, 2293 (2010).
[34]J. Schiøtz and A. E. Carlsson, Philos. Mag. A **80**, 69 (2000).
[35]D. Hull and D. Bacon, *Introduction to Dislocations* (Pergamon Press, Oxford, 1984).
[36]J. Schiøtz, L. M. Canel, and A. E. Carlsson, Phys. Rev. B **55**, 6211 (1997).
[37]K. J. Hsia, Z. Suo, and W. Yang, J. Mech. Phys. Solids **42**, 877 (1994).
[38]See supplementary material at http://dx.doi.org/10.1063/1.4901472 for details of crack propagation under different cases.